JOURNAL OF MATERIALS SCIENCE 37 (2002) 3945–3951

Size distribution of surface cracks and crack pattern in austenitic SUS316 steel plates fatigued by cyclic bending

M. TANAKA, R. KATO
Department of Mechanical Engineering, Akita University, 1-1 Tegatagakuen-cho, Akita 010-8502, Japan
E-mail: tanaka@mech.akita-u.ac.jp

A. KAYAMA
Furukawa Company Ltd., 2-6-1 Marunouchi, Chiyoda-ku, Tokyo 100-0005, Japan

The size distribution of surface cracks and the crack pattern were examined on the specimens of the SUS316 steel plates fatigued by cyclic bending. The size distribution of the cracks could be approximated to a logarithmic normal distribution, irrespective of the maximum total strain range or the number of fatigue cycles. The number of the cracks (Nu) of the length (x') equal to or larger than a given size (X) could be approximated to a power law, $\mathrm{Nu} \propto X^{-a}$, with a scaling exponent a at the larger crack sizes in the fatigued specimens of the SUS316 steel. The value of a decreased with increasing the number of fatigue cycles because of the increase in the number and size of fatigue cracks, and was larger in the specimens tested at the smaller total strain range. Effects of experimental variables on the scaling exponent (a) were also shown in this study. The fractal dimension of spatial crack distribution (the fractal dimension of crack pattern) (D) increased in the range from about 0.9 to about 1.2 with increasing the number of fatigue cycles, and was larger in the specimens fatigued at the larger total strain range. There was a negative correlation between the value of a and the value of D on fatigue cracks, although there was no unique relationship between these two values.

1. Introduction

The growth of a single dominant crack in fatigue has been studied experimentally or theoretically from the viewpoint of fracture mechanics [1]. However, materials fracture is often caused by the growth and linkage of many cracks, and damage mechanics can be applied to the prediction of this type of fracture [2]. The size distribution of the larger cracks seems to be important in this case, since these cracks may lead to final fracture [3]. It is known that the size distribution of creep cracks can be approximated by a logarithmic normal distribution [4, 5]. According to the theoretical study by Mandelbrot [6] and Takayasu [7], one of the present authors analysed the size distribution of creep cracks and revealed that the number of creep cracks (Nu) of the length (x') larger than a given length (X) can be approximated by a power law, $\mathrm{Nu}(x' \geqq X) \propto X^{-a}$, with an exponent a at the larger crack length in a cobalt-base heat-resistant alloy [3]. However, it is not known whether the size distribution of fatigue cracks can be approximated by a similar relationship.

In the fractured specimens of steels [8] and the creep-ruptured specimens of pure Zn polycrystals [9], the size distribution of dimples on the ductile fracture surfaces could be fitted to a power law. The fractal dimension of dimple pattern (D) was close to 1.5 and can be correlated with the scaling exponent of dimple size distribution (a) in these materials. These results imply that the dimple pattern has a morphological feature similar to Sierpinski gasket (the fractal dimension is about 1.58) [10]. In this study, bending fatigue experiments were carried out using the rectangular specimens of the austenitic SUS316 steel. Size distribution of surface cracks was then examined on the fatigued specimens. Effects of experimental variables such as the number of fatigue cycles on the scaling exponent of crack size distribution was also experimentally discussed. Finally, the relationship between the scaling exponent of crack size distribution and the fractal dimension of spatial crack distribution were examined.

2. Experimental procedure

Commercial SUS316 steel plates of 1.5 mm thickness (Fe - 0.06 wt%C - 16.80 wt%Cr - 10.20 wt%Ni - 2.11 wt%Mo - 1.00 wt%Mn - 0.58 wt%Si - 0.027 wt% P - 0.001 wt%S) were used for fatigue experiments in this study. Rectangular specimens of 145 mm length, 10 mm width and 1.5 mm thickness were machined from the steel plates. The specimens were then mechanically polished and finished using diamond paste of 0.25 μm diameter. The average grain diameter of the specimens was 13 μm. Fatigue experiments were

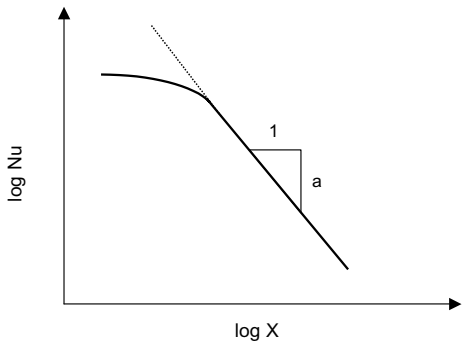

Figure 1 Scaling exponent of crack size distribution, a (Nu: the number of cracks of the size (x') equal to or larger than a given crack length, $X(x' \geqq X)$).

carried out using a bending fatigue equipment by repeatedly bending specimens to cause the maximum total strain range on the broadest specimen surface (the surface area is 10 mm × 145 mm). Therefore, fatigue cracks initiate on the broadest specimen surface and grow in the through-thickness direction. The total strain range has the maximum value at the broadest specimen surface, and the maximum total strain range ($\Delta\varepsilon_t$) was 0.00723, 0.0120 or 0.0169 in this study. The frequency of the fatigue experiments was 0.7 Hz.

The specimens were fatigued to a given number of fatigue cycles (N), and optical micrographs were taken on the surface cracks observed in a given area of 5 mm (in width direction) × 1.6 mm (in length direction) at the central part of the specimen at the magnification of 100 times. The size distribution of fatigue cracks was examined on these micrographs. Scaling exponent of crack size distribution, a, is defined as shown in Fig. 1. As reported in creep of the cobalt-base HS-21 alloy [3], the number of the cracks (Nu) of the size (x') equal to or larger than a given crack length (X) (the cumulative number of the cracks) can be approximated by the following power law with a scaling exponent, a, at the larger crack sizes [6, 7]:

$$\mathrm{Nu}(x' \geqq X) \propto X^{-a} \tag{1}$$

The value of Nu is essentially the ranking of crack size, and the value of X is considered to be the minimum crack length in a given crack size distribution. The fractal dimension of the spatial crack distribution (the fractal dimension of crack pattern) was examined on five micrographs of each specimen, in which crack size distribution was measured. The micrographs were taken into a personal computer by an image scanner, and the cracks in the original images were then manually traced by red lines with one pixel width to obtain the processed images for the fractal analysis [11]. Fig. 2 shows a schematic illustration of the box-counting method used for estimation of the fractal dimension of crack pattern (D). The value of D can be obtained from the following relationship between the number of boxes (n) containing cracks (shown in grey) and the size of boxes (r) [12, 13]:

$$n = n_0 \cdot r^{-D} \tag{2}$$

where n_0 is a constant. The fractal dimension (D) is the averaged value over five images in this study.

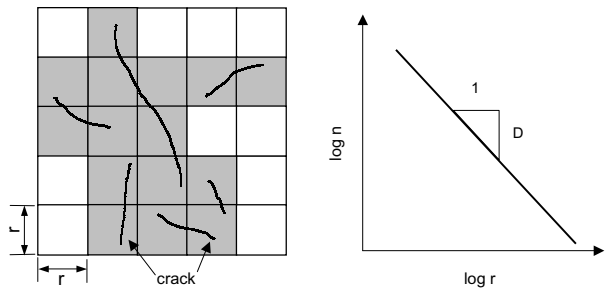

Figure 2 Schematic illustration of the box-counting method (D: the fractal dimension of crack pattern, n: the number of boxes containing cracks, r: the box size).

3. Results and discussion

3.1. Initiation and growth of fatigue cracks

Fig. 3 shows examples of surface cracks observed in the fatigued specimens of the SUS316 steel ($\Delta\varepsilon_t = 0.0120$). The longitudinal direction of the specimens is horizontal. The number of cracks and the crack length increase with increasing the fatigue cycles. The number of fatigue cracks was larger in the specimens tested at the larger value of $\Delta\varepsilon_t$. The large cracks are almost straight and perpendicular to the longitudinal direction (almost normal to the maximum tensile stress), but the shape of the cracks is complex (for example, Fig. 3c and d). Fig. 4 shows examples of fracture surfaces in the fatigued specimens of the SUS316 steel ($\Delta\varepsilon_t = 0.0169$). The macroscopic growth direction of the fatigue crack is horizontal in the micrographs. Stage I fatigue crack growth by slipping-off mechanism occurs from the specimen surface to about 0.2 mm in depth (Fig. 4a), and most of the fracture surface is formed by stage II crack growth with striation patterns (Fig. 4b) [14]. River-like patterns running from the specimen surface, which are composed of many small steps and ledges, are aligned in the macroscopic crack growth direction (Fig. 4a). These patterns are formed by the linkage of fatigue cracks growing on different planes under the effect of mode III loading component. Table I lists the results of fatigue experiments on the SUS316 steel. Fatigue cracks initiated in the early stage of fatigue, and the number of cycles to crack initiation, N_i, is less than 5% of the fatigue life, N_f [14]. The maximum plastic strain range, $\Delta\varepsilon_p$, was calculated using the fracture strain (ε_f) and the fatigue life (N_f) by the following Manson-Coffin type equation [15]:

$$\Delta\varepsilon_p \cdot N_f^{1/2} = \varepsilon_f/2 \tag{3}$$

where ε_f is assumed to be the elongation (0.53) of the SUS316 steel in this study. The calculated value of $\Delta\varepsilon_p$ is 0.00539 for $\Delta\varepsilon_t = 0.0169$, 0.00339 for $\Delta\varepsilon_t = 0.0120$ and 0.00132 for $\Delta\varepsilon_t = 0.00723$.

TABLE I The results of fatigue experiments on the SUS316 steel

$\Delta\varepsilon_t$	N_f	N_i	$\Delta\varepsilon_p$
0.0169	2420	110	0.00539
0.0120	6094	260	0.00339
0.00723	40344	1900	0.00132

$\Delta\varepsilon_t$: the maximum total strain range, N_f: the fatigue life, N_i: the number of cycles to crack initiation, $\Delta\varepsilon_p$: the maximum plastic strain range calculated by Equation 3.

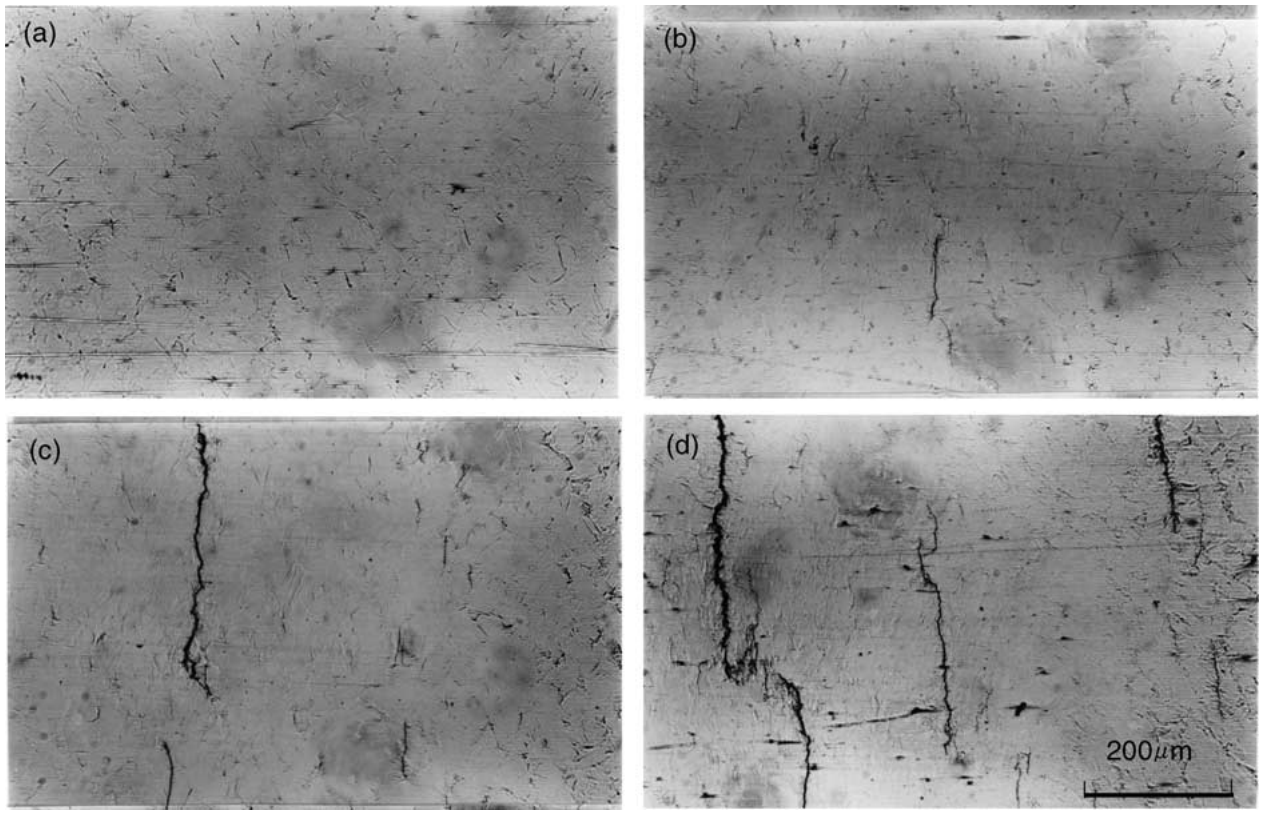

Figure 3 Fatigue cracks observed on the specimen surface of the SUS316 steel fatigued by bending ($\Delta\varepsilon_t = 0.0120$). (a) 1712 cycles, (b) 3164 cycles, (c) 4616 cycles and (d) 6094 cycles (fatigue life).

3.2. Size distribution of fatigue cracks

3.2.1. Scaling exponent of crack size distribution

Fig. 5 shows the size distribution of surface cracks in the fatigued specimens of the SUS316 steel ($\Delta\varepsilon_t = 0.0120$). The size distribution of fatigue cracks can be approximated by the logarithmic normal distribution, irrespective of the number of fatigue cycles. This result is similar to that obtained on the size distribution of creep cracks [4, 5]. The crack size distribution has a long "tail" at the larger crack sizes. Similar results were also obtained on the specimens tested under other conditions. Fig. 6 shows the relationship between the cumulative number of the surface cracks (Nu) (namely, the ranking of crack size) and the crack length (X) in the fatigued specimens ($\Delta\varepsilon_t = 0.0120$). As is known from this figure, the total number of cracks increased in the early stage of fatigue but levelled off in the later stage. The total number of cracks was larger in the specimen tested at the larger value of $\Delta\varepsilon_t$. The value of Nu seems to be well correlated to the value of X by a power law at the crack sizes equal to or larger than about 2.0×10^{-5} m. This value corresponds to the length of fatigue cracks that extended over about twice of the average grain diameter of the specimens (1.3×10^{-5} m). The scaling exponent (a) of crack size distribution can be estimated by fitting the values of Nu and X to Equation 1.

3.2.2. Effects of experimental variables on scaling exponent

The scaling exponent (a) may depend on the fatigue variables or on the materials properties. The following functional dependence of the scaling exponent (a) was assumed in this study:

$$\ln a = \alpha + \beta \ln y + \gamma \ln z \tag{4}$$

$$y = \Delta\varepsilon_p/\varepsilon_r \tag{4a}$$

$$z = (N - N_i)/(N_f - N_i) \tag{4b}$$

where N is the number of fatigue cycles, and parameters α, β and γ are constant for a given value of the minimum crack length (X). The value of y is the normalised plastic strain amplitude, and the value of z is the normalised number of fatigue cycles. The values of α, β and γ were estimated using experimental data by the regression analysis for different values of X. It was found that all the parameters, α, β and γ are negative in the fatigued specimens of the SUS316 steel in this study.

Fig. 7 shows the relationship between the scaling exponent, a, and the normalised number of fatigue cycles, z, in the fatigued specimens for $X = 2.0 \times 10^{-5}$ m. The value of a is larger in the early stage of crack growth, and decreases with increasing the value of z (with increasing the fatigue cycles) because of the increase in the size range of fatigue cracks. This may indicate that the crack initiation as well as the growth and linkage of cracks continues in the fatigue process up to final fracture. The value of a is also larger in the specimens with the same value of z tested at the smaller value of $\Delta\varepsilon_t$ (or $\Delta\varepsilon_p$), in which the number of cracks is smaller. Three curves in the figure are the results of calculations by Equation 4. The values of parameters are $\exp(\alpha) = 0.303$ ($\alpha = -1.19$), $\beta = -0.291$ and $\gamma = -0.727$ for $X = 2.0 \times 10^{-5}$ m. Fig. 8 shows the relationship between the scaling exponent (a) and the normalised fatigue cycles (z) in the specimens of the 316 steel

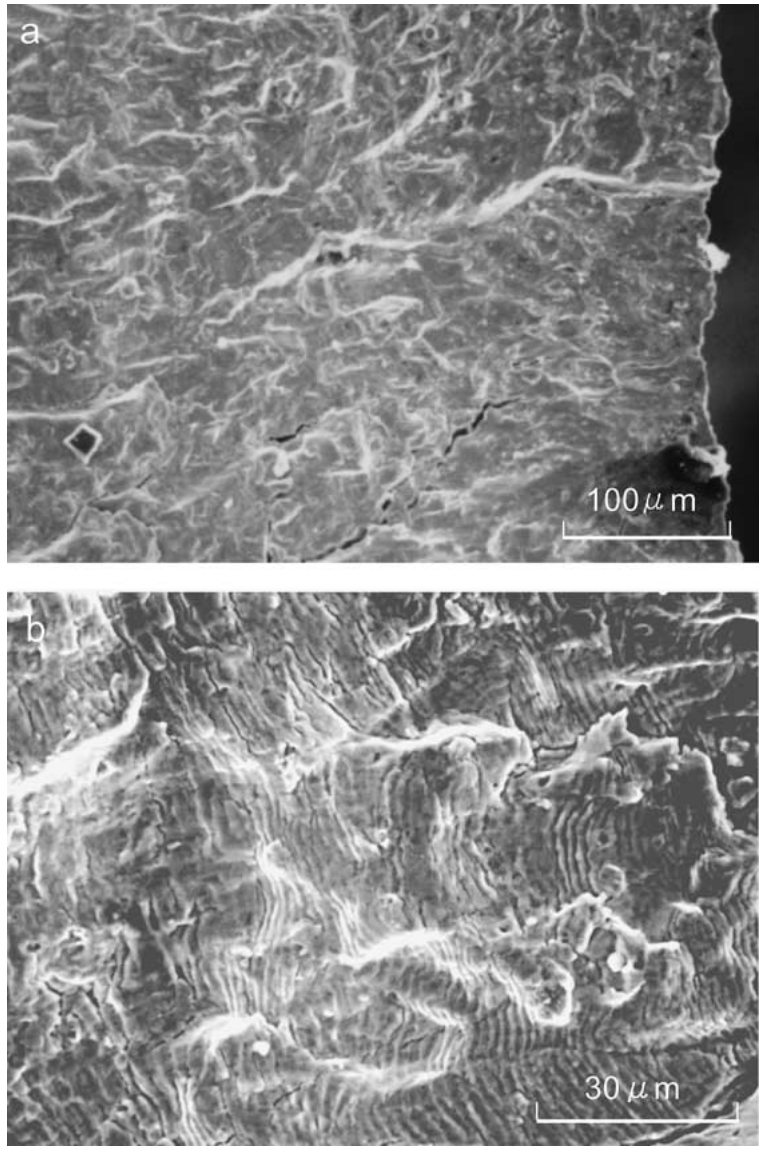

Figure 4 Examples of fracture surfaces in the fatigued specimens of the SUS316 steel ($\Delta\varepsilon_t = 0.0169$). (a) ($x \fallingdotseq 0.2$ mm and (b) $x \fallingdotseq 0.4$ mm (x: the distance from the specimen surface).

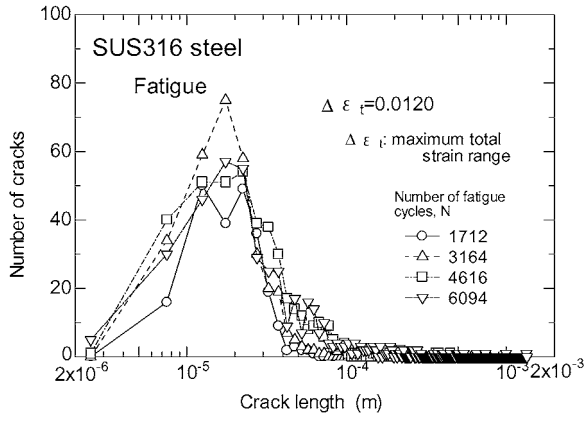

Figure 5 Size distribution of surface cracks in the fatigued specimens of the SUS316 steel ($\Delta\varepsilon_t = 0.0120$).

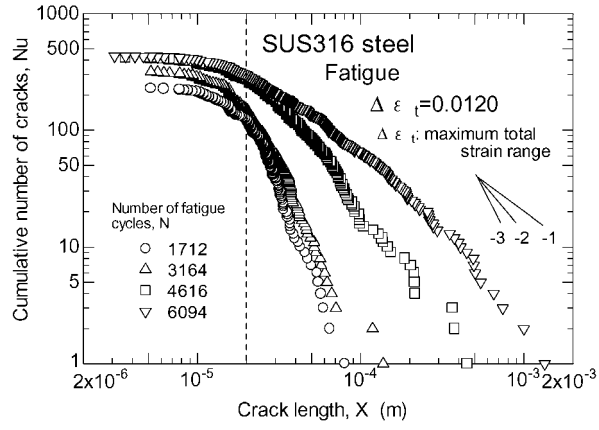

Figure 6 Relationship between the cumulative number of cracks (Nu) and the crack length (X) in the fatigued specimens of the SUS316 steel ($\Delta\varepsilon_t = 0.0120$).

tested at $\Delta\varepsilon_t = 0.0169$). The value of a increases with increasing the value of z (or the fatigue cycles). The scaling exponent (a) tends to increases with increasing the minimum crack length (X). This can be explained in terms of the minimum crack length dependence of the parameters of the scaling exponent. Fig. 9 shows the relationship between the parameters of the scaling exponent (α, β and γ) and the minimum crack length (X) in the fatigued specimens. All the values of the parameters were negative for the SUS316 steel in this study. The value of exp (α) and that of $|\beta|$ depend weakly on the minimum crack size (X) and both values remain almost constant (about 0.3) above the grain size

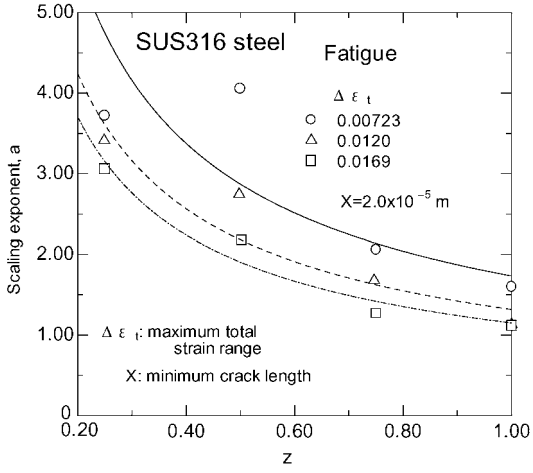

Figure 7 Relationship between the scaling exponent, a, and the normalised number of fatigue cycles, $z(=(N-N_i)/(N_f-N_i))$, in the fatigued specimens of the SUS316 steel.

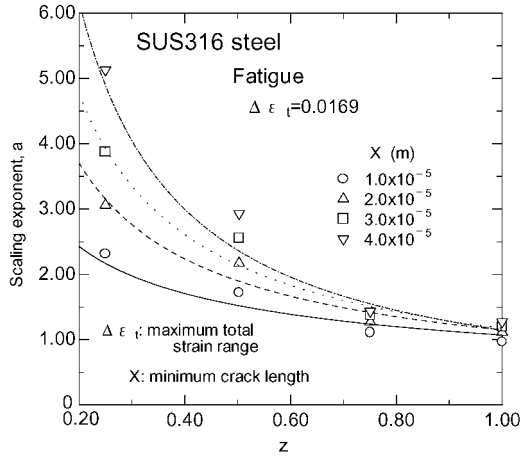

Figure 8 Relationship between the scaling exponent (a) and the normalised number of fatigue cycles (z) in the specimens of the 316 steel tested at $\Delta\varepsilon_t = 0.0169$.

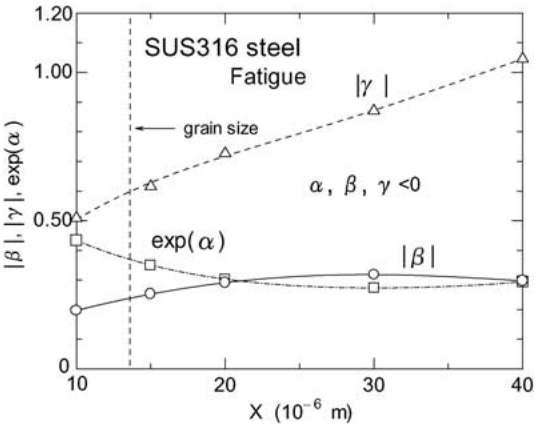

Figure 9 Relationship between the parameters of the scaling exponent and the minimum crack length (X) in the fatigued specimens of the SUS316 steel.

$(1.3 \times 10^{-5}$ m). However, the value of $|\gamma|$ increases from about 0.5 to about 1.0 with increasing the value of X. The increase of the scaling exponent (a) with the minimum crack length (X) is principally attributed to the minimum crack length dependence of the value of γ. Thus, the scaling exponent of crack size distribution (a) depends more strongly on the fatigue cycles (N or z) than on the maximum plastic strain range ($\Delta\varepsilon_p$) in the SUS316 steel.

The scaling exponent (a) may also depend on materials properties that affect the initiation, growth and linkage of fatigue cracks. The dependence of the value of a on the experimental variables may differ in materials with different materials properties. Further study is required to reveal the relationship between the crack size distribution, the experimental variables and the materials properties.

3.3. Spatial distribution and size distribution of fatigue cracks

3.3.1. Fractal nature of spatial crack distribution

Fig. 10 shows examples of the fractal dimension of crack pattern estimated by the box-counting method in the fatigued specimens. The fractal dimension of crack pattern (D) was estimated by fitting the datum points to Equation 2. The value of D increases from about 0.9 to about 1.2 with increasing the number of fatigue cycles. Similar results were obtained in the specimens fatigued under other conditions. Fig. 11 shows the relationship between the fractal dimension of crack pattern, D, and the normalised number of fatigue cycles, $z(=(N-N_i)/(N_f-N_i))$, in the fatigued specimens. The value of D increases with increasing the value of z, and is larger in the specimens tested at the larger

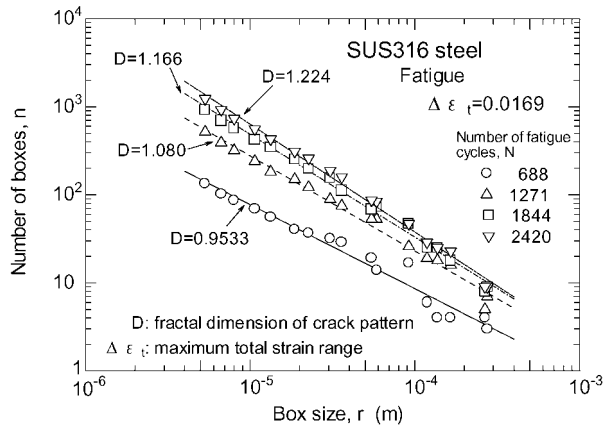

Figure 10 Examples of the fractal dimension of crack pattern estimated by the box-counting method in the fatigued specimens of the SUS316 steel.

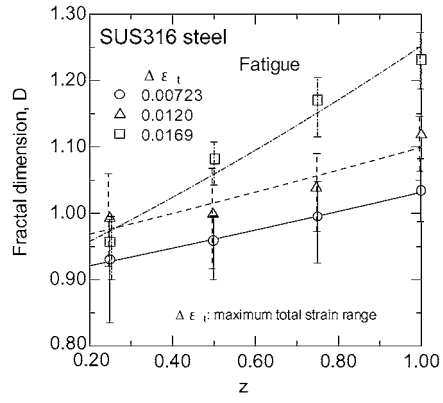

Figure 11 Relationship between the fractal dimension of crack pattern, D, and the normalised number of fatigue cycles, z, in the fatigued specimens of the SUS316 steel.

value of $\Delta\varepsilon_t$. The smallest value of D (about 0.93) lies between the fractal dimension of Cantor dust (about 0.63) and the Euclid dimension of a straight line ($D = 1$) [16]. The largest value of D (about 1.23) is similar to the fractal dimension of Koch curve (about 1.26) [16], although there is no geometrical similarity between the crack pattern and Koch curve.

3.3.2. Relations between size distribution of cracks and crack pattern

Fig. 12 shows the relationship between the fractal dimension of crack pattern (D) and the scaling exponent of crack size distribution (a) (the minimum crack length, $X = 2.0 \times 10^{-5}$ m) in the fatigued specimens. The value of D decreases with increasing the value of a, but three sets of the datum points at different values of $\Delta\varepsilon_t$ are fitted to three separate curves. A unique relationship was not obtained between the fractal dimension (D) and the scaling exponent (a) estimated for all the values of X. The fractal dimension is larger in the specimens tested at the larger value of $\Delta\varepsilon_t$, since the number of surface cracks is larger at the larger value of $\Delta\varepsilon_t$. The value of D may depend not only on the fatigue conditions but also on the materials properties. Fig. 13 shows examples of crack patterns in the specimens fatigue-fractured at different maximum total strain ranges ($\Delta\varepsilon_t$). The scaling exponent of crack size distribution (a) for $X = 2.0 \times 10^{-5}$ m and the fractal dimension of crack pattern (D) are shown in the figure. Two specimens have almost the same values of a but different values of D. As shown in the schematic illustration in the figure, the values of a in two specimens can be almost the same, even if both the number of fatigue cracks (Nu_1, Nu_2) and the length of the largest crack (X_1, X_2) are different.

It is known that the fractal dimension of dimple pattern (D) is about 1.5 and is correlated with the scaling exponent (a) of dimple size distribution (about 1.5) in the fractured specimens of steels [8] or in the creep-ruptured specimens of the pure Zn polycrystals [9]. The dimple pattern on the ductile fracture surface forms a kind of network that is composed of dimple walls

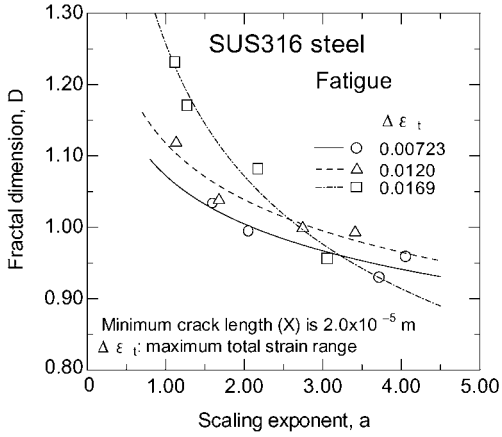

Figure 12 Relationship between the fractal dimension of crack pattern, D, and the scaling exponent of crack size distribution, a, ($X = 2.0 \times 10^{-5}$ m) in the fatigued specimens of the SUS316 steel.

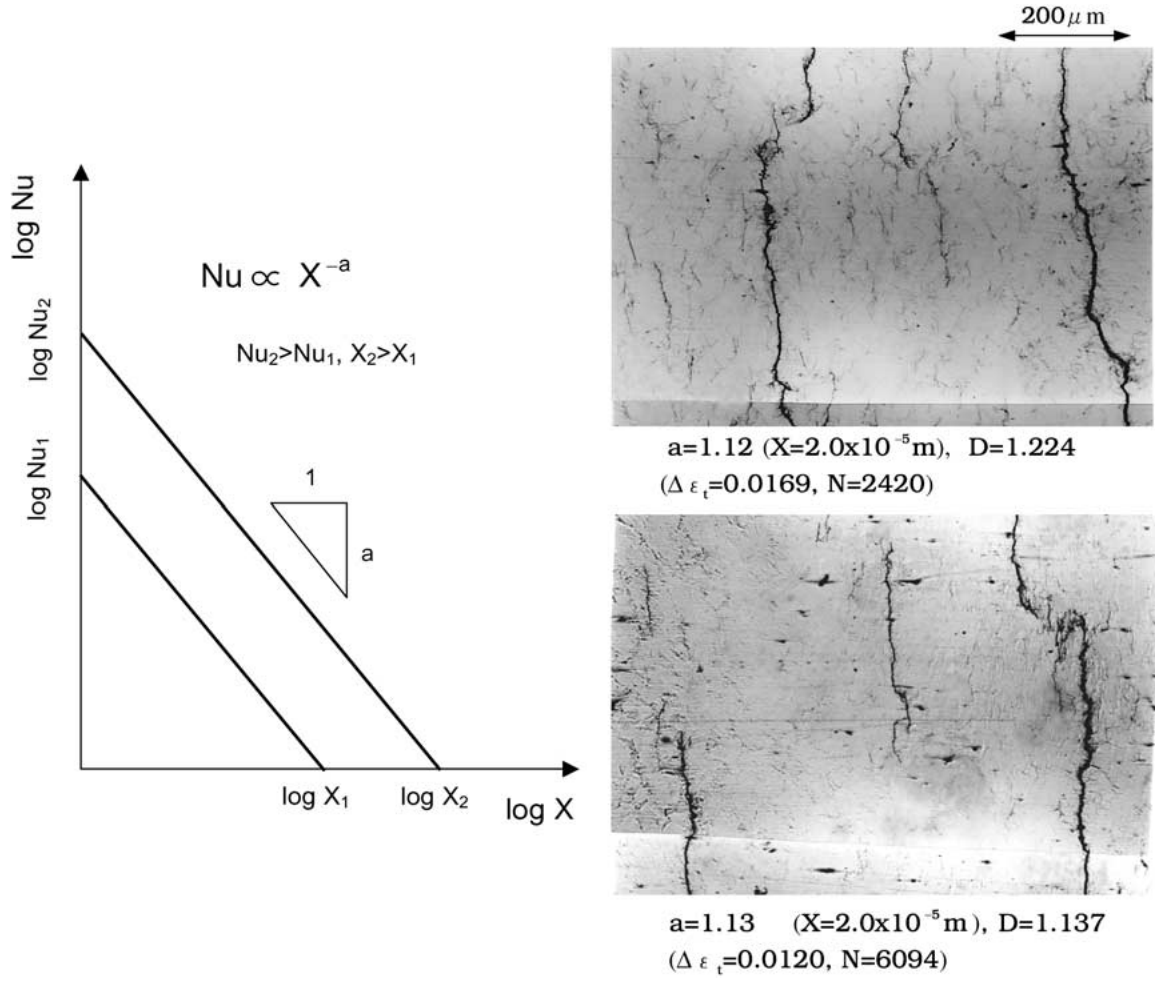

Figure 13 Examples of crack patterns in the specimens fatigue-fractured at different maximum total strain ranges ($\Delta\varepsilon_t$).

[8, 9, 17]. Extensive plastic or creep deformation generally occurs during the growth and linkage of voids, which leads to the formation of dimple pattern on the fracture surface. The formation of dimples is associated with microstructural features such as grain size or population of inclusion [9]. On the other hand, there is a negative correlation between the fractal dimension of crack pattern (D) and the scaling exponent of crack size distribution (a) in the fatigued specimens of the SUS316 steel in this study. There is no unique relationship between the fractal dimension and the scaling exponent about fatigue cracks in the fatigued specimens. Fatigue cracks are discretely spaced on the specimen surface. The larger fatigue cracks grow in the direction almost normal to the maximum tensile stress (the longitudinal direction of a specimen), but the shape of the surface cracks is complex. A large amount of plastic deformation is localised in the near crack-tip region in fatigue, as shown by striations on the fatigue fracture surface (Fig. 4b) [14, 18]. River-like patterns composed of small steps and ledges, which are formed as a result of crack linkage under the effect of mode III loading component, initiated from the specimen surface (Fig. 4a) [14]. These imply that the complex shape of the surface cracks is related to the underlying microstructure in the specimens of the SUS316 steel fatigued by cyclic bending. Thus, differences in the fracture mechanism and the pattern formation may lead to a difference in the fractal nature between the crack pattern and the dimple pattern.

4. Conclusions

The size distribution of surface cracks and the crack patterns were examined on the specimens of the SUS316 plates fatigued by cyclic bending. The results obtained were summarised as follows.

1. The size distribution of the fatigue cracks could be approximated to a logarithmic normal distribution, irrespective of the maximum total strain range ($\Delta\varepsilon_t$) or the number of fatigue cycles (N). The number of the cracks (Nu) of the length (x') equal to or larger than a given size (X) (namely, the ranking of crack size) could be approximated to a power law, $\mathrm{Nu} \propto X^{-a}$, with a scaling exponent a at the larger crack sizes.

2. The value of a decreased with increasing the number of fatigue cycles (N) because of the increase in the size range of fatigue cracks. The value of a was larger in the specimens tested at the smaller total strain range ($\Delta\varepsilon_t$). The dependence of the value of a on the experimental variables were also shown in this study.

3. The fractal dimension of crack pattern (the fractal dimension of spatial crack distribution), D, increased in the range from about 0.9 to about 1.2 with increasing the number of fatigue cycles (N). The value of D was larger in the specimens fatigued at the larger total strain range ($\Delta\varepsilon_t$).

4. There is a negative correlation between the fractal dimension of crack pattern (D) and the scaling exponent of crack size distribution (a) in the fatigued specimens of the SUS316 steel. However, there was no unique relationship between the fractal dimension and the scaling exponent.

Acknowledgments

The authors wish to thank Mr. Y. Kameda and Mr. Y. Nakano for their assistance in experiments. The authors also express their thanks to Sumikin Bussan Co. Ltd. for supplying SUS316 steel plates used in this study.

References

1. K. SADANANDA and P. SHAHINIAN, "Cavities and Cracks in Creep and Fatigue," edited by J. Gittus (Applied Science Publishers, London, 1981) p. 109.
2. D. HULL, "Fractography" (Cambridge University Press, Cambridge, 1999) p. 23.
3. M. TANAKA, *J. Mater. Sci. Lett.* **17** (1998) 91.
4. H. E. EVANS, *Metal Sci. J.* **3** (1969) 33.
5. B. J. CANE and G. W. GREENWOOD, *Metal Sci.* **9** (1973) 55.
6. B. B. MANDELBROT, "The Fractal Geometry of Nature," translated by H. Hironaka (Nikkei Science, Tokyo, 1985) p. 20.
7. H. TAKAYASU, "Fractals in the Physical Sciences" (Manchester University Press, Manchester, 1990) p. 11.
8. K. ISHIKAWA, *J. Mater. Sci. Lett.* **9** (1990) 400.
9. M. TANAKA, *ibid.* **17** (1998) 1715.
10. B. B. MANDELBROT, "The Fractal Geometry of Nature," translated by H. Hironaka (Nikkei Science, Tokyo, 1985) p. 130.
11. X. W. LI, J. F. TIAN, Y. KANG and Z. G. WANG, *Scripta Metall. Mater.* **33** (1995) 803.
12. B. B. MANDELBROT, "The Fractal Geometry of Nature," translated by H. Hironaka (Nikkei Science, Tokyo, 1985) p. 280.
13. H. TAKAYASU, "Fractals in the Physical Sciences" (Manchester University Press, Manchester, 1990) p. 123.
14. M. TANAKA, A. KAYAMA, R. KATO and A. MUTO, *Key Engineering Materials* **145–149** (1998) 107.
15. G. E. DIETER, "Mechanical Metallurgy" (McGraw-Hill Kogakusha, Tokyo, 1976) p. 413.
16. B. B. MANDELBROT, "The Fractal Geometry of Nature," translated by H. Hironaka (Nikkei Science, Tokyo, 1985) p. 440.
17. D. HULL, "Fractography" (Cambridge University Press, Cambridge, 1999) p. 234.
18. *Idem.*, "Fractography" (Cambridge University Press, Cambridge, 1999) p. 259.

Received 19 June 2001
and accepted 27 March 2002